1521-0103/382/3/266–276$35.00
THE JOURNAL OF PHARMACOLOGY AND EXPERIMENTAL THERAPEUTICS

dx.doi.org/10.1124/jpet.121.001067
J Pharmacol Exp Ther 382:266–276, September 2022

The Journal of PHARMACOLOGY And Experimental Therapeutics

Effect of Novel Biotherapeutic Elevating Angiopoietin 1 on Progression of Diabetic Nephropathy in Diabetic/Obese Mice[S]

Peng Sun,[1] Christina S. Bartlett,[1] Chao Zheng, Tammy Bigwarfe, Joshuaine M. Grant, Margit MacDougall, Valentina Berger, Steven Kerr, Hu Sheng Qian, Mark McHugh, Hongxing Chen, Xiaomei Zhang, Miranda L. Carpenter, Heather N. Robinson, John Miglietta, Thorsten Lamla, and Ryan M. Fryer

Cardiometabolic Diseases Research (P.S., C.S.B., M.Ma., V.B., S.K., H.S.Q., M.Mc., H.C., X.Z., M.L.C., H.N.R., R.M.F.), Biotherapeutic Discovery (C.Z., J.M.), Biotherapeutic Pharmacokinetics (T.B., J.M.G.), and Target Discovery Research (T.L.), Boehringer Ingelheim Pharmaceuticals, Inc., Ridgefield, Connecticut

Received December 20, 2021; accepted June 14, 2022

ABSTRACT

Diabetic nephropathy is a leading cause of end-stage renal disease, characterized by endothelial dysfunction and a compromised glomerular permeability barrier. Dysregulation of the angiopoietin 1 (ANGPT1)/angiopoietin 2 (ANGPT2) signaling axis is implicated in disease progression. We recently described the discovery of an IgG_1 antibody, O010, with therapeutic potential to elevate circulating endogenous ANGPT1, a tyrosine kinase with Ig and epidermal growth factor (EGF) homology domains-2 (TIE2) agonist. Studies are described that detail the effect of various ANGPT1-elevating strategies to limit progression of renal dysfunction in diabetic-obese (db/db) mice. Results demonstrate that adeno-associated virus– or DNA minicircle–directed overexpression of ANGPT1 elicits a reduction in albuminuria (56%–73%) and an improvement in histopathology score (18% reduction in glomerulosclerosis). An improved acetylcholine response in isolated aortic rings was also observed indicative of a benefit on vascular function. In separate pharmacokinetic studies, an efficacious dose of the ANGPT1 DNA minicircle increased circulating levels of the protein by >80%, resulting in a concomitant suppression of ANGPT2. At a dose of O010-producing maximal elevation of circulating ANGPT1 achievable with the molecule (60% increase), no suppression of ANGPT2 was observed in db/db mice, suggesting insufficient pathway engagement; no reduction in albuminuria or improvement in histopathological outcomes were observed. To pinpoint the mechanism resulting in lack of efficacy, we demonstrate, using confocal microscopy, an interference with TIE2 translocation to adherens junctions, resulting in a loss of protection against vascular permeability normally conferred by ANGPT1. Results demonstrated the essential importance of ANGPT1 to maintain the glomerular permeability barrier, and, due to interference of O010 with this process, led to the discontinuation of the molecule for clinical development.

SIGNIFICANCE STATEMENT

This body of original research demonstrates that elevation of systemic angiopoietin 1 (ANGPT1) is protective against diabetic nephropathy. However, using a novel biotherapeutic approach to elevate systemic ANGPT1 renoprotection was not observed; we demonstrate that protection was lost due to interference of the therapeutic with ANGPT1/ tyrosine kinase with Ig and EGF homology domains-2 translocation to adherens junctions. Thus, the clinical development of the antibody was terminated.

Introduction

In a pivotal paper using untargeted proteomic profiling of circulating proteins from patients with diabetes, the "Joslin Kidney Study," elevated plasma angiopoietin 1 (ANGPT1) was associated with protection against progressive renal decline and progression of end-stage renal disease (Md Dom et al., 2021). ANGPT1 is a 70-kD glycoprotein and the major agonist for tyrosine kinase with Ig and EGF homology domains-2 (TIE2), expressed primarily on endothelial cells including glomerular endothelial cells (Davis et al., 1996; Satchell et al., 2002). ANGPT1 is required to maintain endothelial cell quiescence, promote restoration of vascular function, and regulate vascular permeability (Uemura et al., 2002). In contrast, angiopoietin 2 (ANGPT2), released from Weibel-Palade bodies

This work received no external funding.
All authors were employed at Boehringer Ingelheim Pharmaceuticals at the time the research was performed. No author has an actual or perceived conflict of interest with the contents of this article.
[1]P.S. and C.S.B. contributed equally to this work as first authors.
dx.doi.org/10.1124/jpet.121.001067.
[S] This article has supplemental material available at jpet.aspetjournals.org.

ABBREVIATIONS: AAV, adeno-associated virus; ANGPT1, angiopoietin 1; ANGPT2, angiopoietin 2; CKD, chronic kidney disease; COMP-Ang1, chimeric protein of cartilage oligomeric matrix protein and angiopoietin 1; db/db, diabetic-obese; DN, diabetic nephropathy; ECL, electrochemiluminescence; EGF, epidermal growth factor; EGM-2, endothelial cell growth medium-2; FOXO1, forkhead box protein O1; HUVEC, human umbilical vein endothelial cell; MC, minicircle; MSD, Meso Scale Discovery; PAM, periodic acid methenamine silver; RT, resting tension; TIE2, tyrosine kinase with Ig and EGF homology domains-2; TNFα, tumor necrosis factor α; UACR, urinary albumin-to-creatinine ratio; UAE, urinary albumin excretion; UNx, uni-nephrectomy; VE, vascular endothelial.

(Fiedler et al., 2004), is a functional antagonist of ANPGT1 binding to TIE2, thereby inhibiting TIE2 signaling, and thus promotes endothelial activation, destabilization, and vascular leakage (Fiedler and Augustin, 2006).

In diabetic nephropathy (DN), a leading cause of end-stage renal disease worldwide (Bell et al., 2015; Ghaderian et al., 2015), it has been suggested that there is dysregulation of the ANGPT1-ANGPT2-TIE2 axis in disease, both in humans and in preclinical models. Circulating ANGPT1 is decreased and ANGPT2 is elevated in chronic kidney disease (CKD) patients with moderately to severely reduced glomerular filtration rates (Futrakul et al., 2008). Intriguingly, ANGPT2 expression is negatively regulated via an ANGPT1-TIE2 downstream signaling pathway through AKT (protein kinase b) and forkhead box protein O1 (FOXO1) in human endothelial cells (Daly et al., 2004). Thus, reduced ANGPT1 in disease may be permissive for ANGPT2 synthesis, further exacerbating endothelial dysfunction in CKD. Similarly, in animal models of kidney disease, ANGPT1 is reduced and correlated with increased glomerulosclerosis and albuminuria (Yuan et al., 2002; Jeansson et al., 2011), suggesting a conserved disease etiology in rodents.

ANGPT1 may be especially important in the context of maintaining renal function given its predominant cortical expression in podocytes and juxtaposition to glomerular endothelia. Exquisite studies in healthy adult podocytes using high-power multiplexed immunofluorescence analyses in combination with immunohistochemical analyses demonstrate clear podocyte ANGPT1 expression in the foot process, colocalized with nephrin, whereas Tie2 is predominantly expressed in the glomerular endothelium, particularly on the abluminal surface (Satchell et al., 2002). The cellular localization of these proteins lends to the stabilization of the glomerular capillary structure (to reduce permeability), especially at adherens junctions, and thus limit protein leak into the urine under normal conditions. Indeed, in diabetic mice, podocyte-specific deletion of ANGPT1 exacerbates glomerular damage and precipitates proteinuria (Jeansson et al., 2011).

Thus, enhancing ANGPT1-TIE2 signaling to restore endothelial function in CKD may offer promising therapeutic potential to reverse the course of disease. Unfortunately, the magnitude of increase in circulating ANGPT1 necessary to stimulate glomerular endothelial TIE2 and reverse the pathology is unclear. This is compounded by the difficulty of accurately measuring ANGPT1 in circulation due to ex vivo activation of platelets that may have artificially confounded values reported in previous clinical studies (Reed and Schrier, 2011).

Previously, we reported the discovery of a novel IgG_1-based molecule that selectively increases circulating ANGPT1 by binding to and stabilizing ANGPT1 at an epitope outside the TIE2 binding domain. We also demonstrated proof of concept that the same molecule, termed O010, significantly elevates circulating levels of the protein in cynomolgus monkeys after a single injection of the antibody (Zheng et al., 2018).

Building on these observations, we use different strategies to overexpress ANGPT1 in the circulation and test the impact of elevated ANGPT1 protein on progression to kidney disease in mice. Furthermore, we define the necessary circulating ANGPT1 levels that successfully restored renal and vascular function and tested the effect of the ANGPT1-elevating antibody, O010, for proof of concept to reduce renal dysfunction and support advancement into clinical development.

Materials and Methods

Materials (Antibody, DNA Minicircle, Adeno-Associated Virus)

Mouse ANGPT1 minicircle was obtained from System Biosciences (Palo Alto, CA). The ANGPT1 antibody O010 and the IgG control antibody were produced at Boehringer Ingelheim Pharmaceuticals as previously disclosed (Zheng et al., 2018). The chimeric protein of cartilage oligomeric matrix protein and angiopoietin 1 (COMP-Ang1) adeno-associated virus (AAV) (Cho et al., 2004) was produced as follows: a synthetic piece of DNA containing a Kozak sequence followed by a secretory signal sequence for hemagglutinin, the coiled-coil domain of rat cartilage oligomeric matrix protein fused to the fibrinogen-like domain of human ANGPT1 (Cho et al., 2004) and a WPRE (Woodchuck hepatitis virus posttranscriptional regulatory element) sequence was synthesized at GeneArt (Regensburg, Germany) and cloned into the plasmid for adenoassociated virus (pAAV)-multiple cloning site (MCS) (Agilent Technologies, catalog no. 240071) without β-globin intron (Aschauer et al., 2013) via the ClaI and BglII restriction sites and termed pAAV_CMV-COMP-ANGPT1. The pAAV-Stuffer (Strobel et al., 2015) was used as a control. A commercially available packaging plasmid consisting of AAV2 rep, AAV8 cap, and Ad5 helper function (PlasmidFactory, catalog no. pDPape8) was used for packaging the recombinant AAV (rAAV) constructs containing AAV2-ITRs into an AAV8 capsid. The rAAV8 vectors were produced as described previously (Aschauer et al., 2013).

Measurement of ANGPT1 and ANPGT2 in Plasma

ANGPT2 plasma concentrations were measured using mouse/rat quantikine ELISA kits (R&D Systems) per the manufacturer's instructions. ANGPT1 plasma concentrations were measured using a Meso Scale Discovery (MSD) assay. Briefly, gold small spot streptavidin plates (MSD part #L45SA) were coated with 1 μg/mL biotinylated mouse monoclonal antihuman ANGPT1 antibodies (R&D Systems, MAB9231), then incubated overnight at 2–8°C. The plates were washed (1X PBS with 0.05% Tween 20) then blocked with 5% bovine serum albumin (BSA) (SeraCare) containing 0.05% Tween 20. Following incubation for 1 hour at ambient temperature, plates were washed and reference standard (recombinant mouse ANGPT1 protein, R&D Systems) and test samples diluted 2× in MSD diluent 7 were added for 2 hours at ambient temperature. The plates were washed and MSD Sulfo-labeled polyclonal goat antihuman ANGPT1 (R&D Systems, AF923) diluted to 1 μg/mL with MSD diluent 3 was added and incubated for 2 hours at ambient temperature. After washing, 2× MSD Read Buffer was added and the electrochemiluminescence (ECL) signal was then measured on a Sector Imager 6000 instrument. Analyte concentrations were determined from data regression of the ECL signal converted to concentration values. Quantitation was based on a four-parameter logistic ($1/Y^2$) regression equation from reference standard curves generated using the MSD Discovery Workbench software.

Western Blot

Kidney cortices from mice were homogenized using immunoprecipitation (IP) Lysis Buffer containing Halt Protease and Phosphatase Inhibitors with Lysing Matrix D tubes on an MP Fastprep-24 5G Instrument. Protein (BCA) quantification was determined and samples were normalized to 1 mg/mL for immunoprecipitation overnight rotating at 4°C with 4 μg of mouse/rat Tie-2 antibody (R&D Systems AF762). 50 μg of protein were used for polyacrylamide gel electrophoresis, transferred to 0.45 μm nitrocellulose membranes, and incubated with 5% skim milk before incubating with antibodies.

The anti-TIE2 (phospho Y1102) antibody ab111585 (1:50) was used to detect phosphorylation; mouse/rat Tie-2 antibody (R&D Systems

AF762, 0.1 μg/mL) was used for total TIE2 immunoprecipitation and IgG heavy chain as a loading control.

The membrane was washed three times with Tris buffered saline with Tween20 (TBST) and incubated with secondary antibodies (1:5000 dilution) at room temperature for 1 hour. The membranes were washed again and subjected to ECL detection.

In Vivo Pharmacology

All in vivo experiments were conducted in compliance with the rules set forth by the Boehringer Ingelheim Institutional Animal Use and Care Committee in accordance with the guidelines established in the National Institutes of Health's Guide for the Care and Use of Laboratory Animals (https://www.ncbi.nlm.nih.gov/books/NBK54050/pdf/Bookshelf_NBK54050.pdf). Studies were conducted in Boehringer Ingelheim's International, Association for the Assessment and Accreditation of Laboratory Animal Care–accredited facility.

Male db/db mice and their controls, vehicle mice, were purchased from Charles River Laboratories (Kingston, NY) at 7–8 weeks of age with or without uninephrectomy performed at 5 weeks of age, as detailed in the *Results*. Mice were acclimated for 3 days upon arrival and were housed in groups of two to three per cage with a 12-hour light-dark cycle and ad libitum access to food and water. All in vivo studies were designed in a similar fashion; any notable differences are described in the *Results*. In brief, mice were randomly assigned to treatment groups based on average baseline urinary albumin excretion (UAE) and body weight. Mice were single-housed in metabolic cages for urine collection; blood samples were collected from the jugular vein (interim time point) or cardiac puncture (terminal time point) for purposes of measuring soluble factors or antibody PK. At study termination, mice were sacrificed by exsanguination through cardiac puncture under isoflurane anesthesia, and tissues were collected for ex vivo, histologic, or other relevant analyses as detailed in the *Results* section.

Histology

Tissue Collection and Processing. For histologic assessment, kidneys were removed and weighed, and a midorgan transverse section of the left kidney was collected and immediately fixed by immersion in 10% phosphate-buffered formalin for 48 hours. Subsequently, formalin-fixed tissues were washed in phosphate buffer, dehydrated through a graded series of ethanol and xylene, embedded in paraffin, and sectioned at 4 μm.

General Assessment of Renal Histopathology. Kidney tissue sections (4 μm) were stained with periodic acid methenamine silver for the general assessment of incidence of glomerulosclerosis and H&E for the general assessment of total number of foci of interstitial lesions. For the glomerular lesions, the number of glomeruli showing mild-to-severe glomerulosclerosis was counted in each kidney section and expressed as a percentage of the total glomerular population. Tubulointerstitial lesions were assessed as the number of foci showing obvious renal damage, which included marked hypercellularity (inflammation or resident myofibroblast increases), fibrosis, tubular hyperplasia, casts, or necrosis. Both assessments were performed under blinded conditions at 10× magnification.

Immunohistochemistry and Quantification of Glomerular Podocytes. 4 μm kidney sections were air dried overnight at 37°C, dewaxed, and rehydrated in graded ethanol to phosphate-buffered saline. Endogenous peroxidase activity was blocked by ImmPRESS (Vector Laboratories; Burlingame, CA) for 20 minutes at ambient temperature. Sections were then washed and incubated with the primary antibody for p57 (tissue marker of glomerular podocyte, sc8298; Santa Cruz; Dallas, TX) at a dilution of 1:500 and were subsequently incubated with the respective secondary antibodies (ImmPress Reagent Kit; Vector Laboratories) for 30 minutes in a hydration chamber. Immunoperoxidase detection was performed using the avidin-biotin complex method (Vector Laboratories) using 3,3′-diaminobenzidine tetrahydrochloride as substrate. Quantification of glomerular podocyte was performed under blinded conditions. Thirty random digital images were captured at 20× objective magnification, and the number of podocytes or the cell number with positive expressed p57 for each individual glomeruli was counted manually for all 30 images and the final result was calculated as average number of podocyte per glomeruli.

Aortic Ring

Aortic rings from mouse aortas of ~2 mm in length were cleaned of adherent connective tissue, isolated, and immediately transferred into a chilled (4°C) Krebs' solution composed of $CaCl_2$ (anhydrous) 0.28g; $NaHCO_3$, 2.1g; HEPES, 1M; and Kreb's powder (Krebs-Henseleit Buffer modified, K3753-10x1L). Kreb's was previously bubbled with a mix of gases containing 95% O_2 and 5% CO_2 to pH 7.4. Aortic rings were mounted into a wire myograph system. Each ring was placed on two wire hooks in block-heated tissue baths containing 8 mL of the same Krebs' solution kept at 37°C and constantly bubbled with 95% O_2 and 5% CO_2. The upper hook was connected to a force transducer to detect changes in isometric force. Changes in isometric force were continuously recorded using Chart 5.4 (PowerLab, AD Instruments Inc.; North America). Passive tension was set to 1.55 g and all subsequent measurements representing the force were generated above this baseline. A 1-hour equilibration period was applied before any experimental intervention, during which the bath was flushed with fresh Krebs' solution every 30 minutes. After equilibration, the aortic rings were tested with a single dose of KCl (50 mM) to confirm smooth muscle viability. After maximal contraction was reached, the tissue baths were washed with fresh Krebs solution three times and left to re-equilibrate for another 20 minutes. Following relaxation back to baseline, the tissues were preconstricted with phenylephrine at a concentration of 10^{-6} M. The vessels were allowed to constrict to the maximum response to phenylephrine, then a cumulative dose-response curve with acetylcholine was performed at the following concentrations: 10^{-9}, 3×10^{-9}, 10^{-8}, 3×10^{-8}, 10^{-7}, 3×10^{-7},1×10^{-6}, 3×10^{-6}, 1×10^{-5}M. Analysis of the EC_{50} for each dose-response cure was performed and the EC_{50} determined using GraphPad Prism 9 software [data transformed into logarithmic scale values (X = 1e−9*X) and then X = log(X)] and the EC_{50} determined using nonlinear regression (curve fit) dose-response inhibition [Log(inhibitor) versus response−variable slope (four parameters) (Formula: Y = Bottom + (Top−Bottom)/(1 + 10^((LogIC50−X)*HillSlope)].

Phospho-TIE2 Localization

Pooled donor human umbilical vein endothelial cells (HUVECs) (Lonza, CC-2519A) were cultured in endothelial cell growth medium-2 (EGM-2) media according to manufacturer instructions. To determine the effect of ANGPT1 non-neutralizing antibodies on phosphorylated TIE2 localization, passage 3 HUVECs were plated on collagen I–coated chamber slides (Corning, 354630) at a density of 30,000 cells per well. Cells were switched into starvation media 4 hours post plating. The following morning, HUVECs were stimulated with starvation media containing 500 ng/mL recombinant human ANGPT1 (BIPI ID PW.PR.00346095, lot FHW381501A) with or without 100 nM non-neutralizing

ANGPT1 antibodies (O010, BIPI ID PW.PR.00349790, lot dliu3_20161018_090.3CEX) for 30 minutes at 37°C. Media was aspirated and cells were fixed with 4% paraformaldehyde for 15 minutes at 4°C. Cells were washed in phosphate-buffered saline, permeabilized with 0.05% TritonX-100, and washed again prior to blockade in 1% BSA, 10% donkey serum in phosphate-buffered saline. Slides were incubated in primary antibodies for phospho-TIE2 (Y992; R&D Systems, AF2720, 1:25) and vascular endothelial (VE)-cadherin (R&D Systems, MAB9381, 1:500) overnight in blocking solution at 4°C. The following day, slides were washed in PBS and incubated in secondary antibodies (anti-rabbit Alexa488, anti-mouse Alexa594; Invitrogen) in blocking solution for 60 minutes at room temperature in the dark, stained with 4′,6-diamidino-2-phenylindole (DAPI) and mounted with SlowFade Diamond (ThermoFisher, S36967). Slides were imaged using 20× magnification on an LSM 880, AxioObserver Zeiss confocal microscope.

Images were processed using Fiji-ImageJ. To quantify the junctional pTIE2, the VE-cadherin channel was converted to a binary image for generation of a mask that was overlaid onto the pTIE2 image, allowing for quantification of pTIE2 signal localized within the adherens junctions. The area, mean density and integrated densities were captured from each well. Each experiment contained 3–9 well replicates, and two independent experiments were performed.

Permeability Assay

Pooled donor HUVECs (Lonza, CC-2519A) were cultured in EGM-2 media and evaluated using the In Vitro Vascular Permeability Assay following manufacturer instructions (96-well; Millipore, ECM642). Briefly, 50,000 HUVECs were seeded onto prehydrated collagen I–coated inserts in 100 μL of EGM-2 media and the receiver was filled with 250 μL of EGM-2. Cells were incubated for 48 hours prior to stimulation with vascular permeability factors [10 ng/mL tumor necrosis factor-α (TNFα) (EMDMillipore, GF442), 200 ng/mL ANGPT1, and 100 nM O010 or IgG1 control antibody]. After 24 hours, media containing permeability factors was removed and 75μL of a 1:40 fluorescein isothiocyanate (FITC)-Dextran solution in EGM-2 was added to the

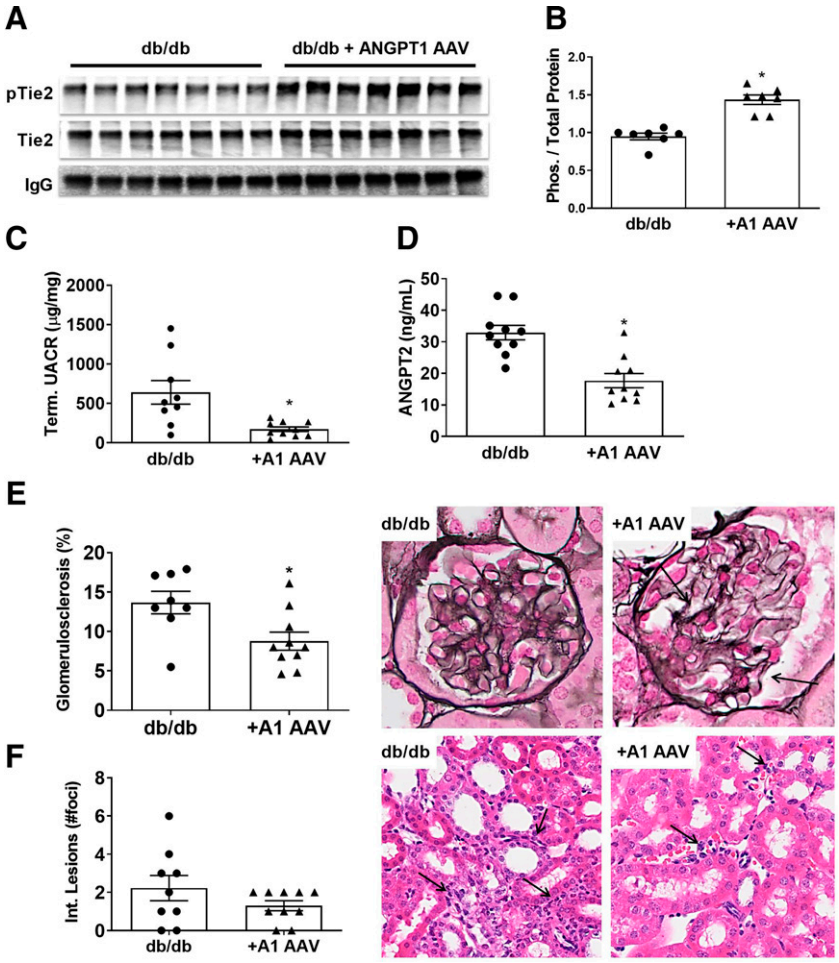

Fig. 1. Transfection of db/db mice with AAV to overexpress COMP-Ang1 (A1 AAV). Overexpression of ANGPT1 (A and B) increased renal cortical phosphorylation of TIE2 and (C) reduced leakage of albumin into the urine as shown by a decreased UACR at 10 weeks post-AAV. (D) ANPGT2 levels were reduced in the presence of ANGPT1-AAV, suggesting signaling through the FOXO pathway to downregulate ANPGT2 expression. (E and F) By histologic assessment, ANGPT1-AAV significantly reduced the incidence of glomerular lesions; reductions in the number of interstitial lesions were not statistically significant. Glomerular lesions stained black by periodic acid methenamine silver (PAM): db/db glomerulus shows expanded matrix throughout the mesangium and the A1 AAV shows mesangial matrix in one-fourth of the glomerular area (arrows). Lesions in mice treated with the A1 AAV were fewer and appeared less severe than those observed in db/db mice. Interstitial lesions were stained by H&E: db/db mice present with interstitial cellularity (arrows) while matrix expansion or fibrosis was not observed. The A1 AAV mice showed fewer foci and less cellularity relative to db/db mice. Areas of cellularity were typically associated with tubular dilation.

insert and placed in 250 μL of EGM-2 in the receiver tray. Permeation continued for 20 minutes, after which the inserts were removed, media in the receiver tray was mixed by pipetting, and 100 μL was transferred to a black-walled opaque plate. Fluorescence was measured on a SpectraMax 5 with 485 nm excitation and 535 nm emission filters, using 4 replicates per group per experiment. Two independent experiments were performed, and the data are presented as the relative fluorescence units in the receiver well ± S.E.M. from one experiment.

Statistical Analysis

As appropriate, experimental results are shown both as individual data points and mean ± S.E.M. Since more than one statistical method was used based on the experimental conditions or comparator groups, the specific statistical test performed is detailed within the results for each experiment or set of data.

Results

Effect of ANGPT1 Overexpression Using COMP-Ang1 AAV on DN Progression in db/db Mice (Fig. 1)

The ANGPT1 variant, COMP-Ang1, has been previously characterized as an ANGPT1-like TIE2 agonist to promote receptor signaling in vivo (Kim et al., 2008; Ryu et al., 2015). In the present study, COMP-Ang1 AAV was delivered via tail vein injection to db/db mice at 1×10^{10} vector genomes per mouse, and mice were euthanized 8 weeks postinjection. COMP-Ang1 injection resulted in a 51.2% increase in renal TIE2 phosphorylation (pTIE2) as compared with the control group (Fig. 1, A and B). The summarized data (Fig. 1B) are presented as the junctional pTIE2 integrated density for individual lanes as well as mean ± S.E.M. To test for statistical significance ($P < 0.05$), a Student's t test (unpaired, two-tailed) was performed.

The enhancement of ANGPT1-TIE2 signaling by COMP-Ang1 in the kidney significantly reduced the terminal urinary albumin-to-creatinine ratio (UACR) by 72.9% (Fig. 1C) and circulating ANGPT2 by 46.2% (Fig. 1D) in contrast to control group. Treatment ameliorated glomerulosclerosis by 36.9% (Fig. 1E) and reduced interstitial lesions by 41.5% (Fig. 1F). Results are shown from individual animals as well as mean ± S.E.M. To test for statistical significance ($P < 0.05$), a Student's t test (unpaired, two-tailed) was performed. Representative histology images are also shown from an animal with glomerulosclerosis and interstitial lesion scores closest to the group mean (Fig. 1, E and F).

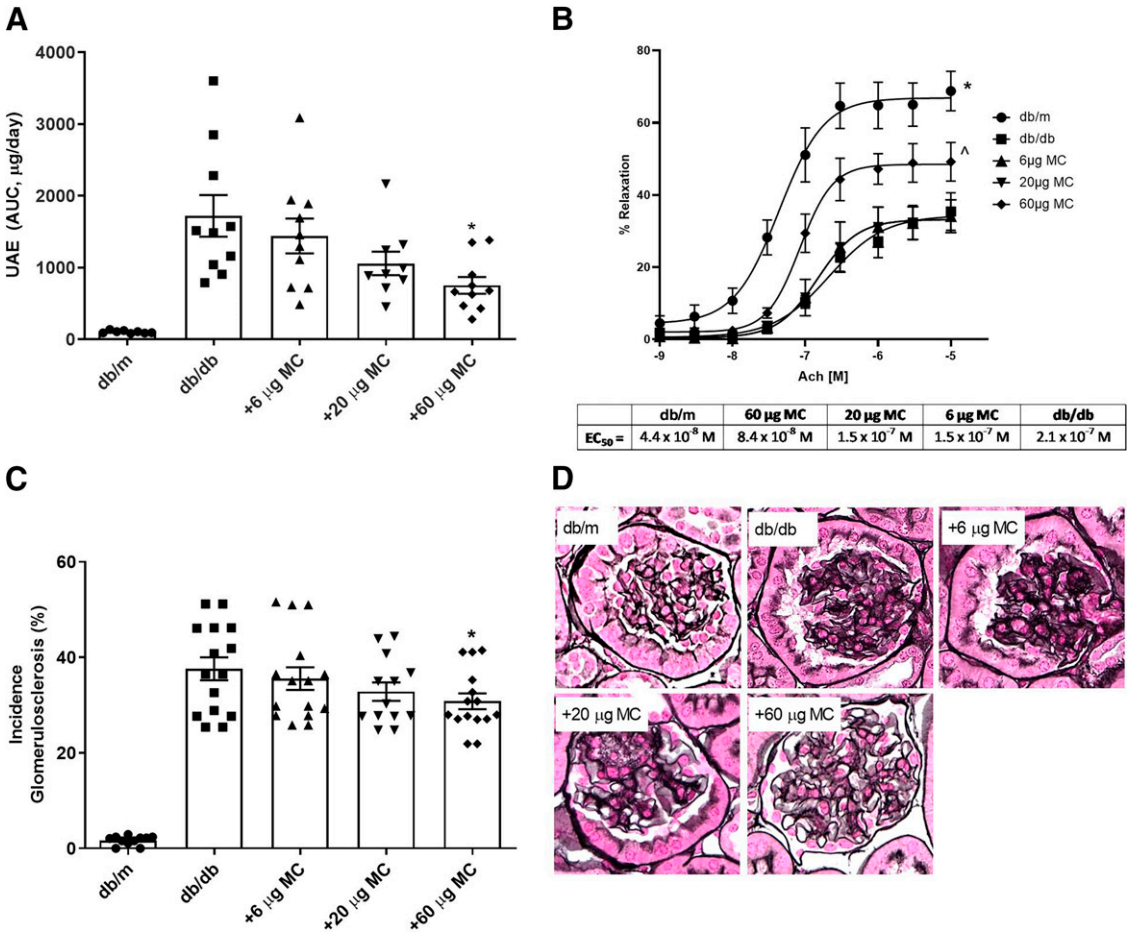

Fig. 2. Effect of ANGPT1 elevation using DNA-minicircle on the excretion of albumin. (A) Results are shown as an AUC for the duration of the study where 60-μg treatment reduced the UAE significantly in contrast to vehicle control group. (B) DNA-Minicircle overexpression of ANGPT1 also significantly improved vascular function in isolated aortic rings. (C and D) The incidence of glomerulosclerosis was markedly increased in db/db mice relative to vehicle controls. After treatment with ANGPT1 MC, there was a trend for a dose-dependent reduction in incidence of glomerulosclerosis when compared with db/db mice. However, only db/db mice treated with 60 μg of MC reached statistical significance. db/m, vehicle.

Dose-Responsive Elevation of ANGPT1 Using DNA-Minicircle and Effect on DN Progression in db/db Mice (Fig. 2)

The effect of elevated ANPGT1 was tested using DNA minicircle in db/db mice with uninephrectomy to accelerate DN progression. Three doses of the ANGPT1 minicircle (6, 20, and 60 μg/mouse) or a control minicircle was delivered via hydrodynamic injection. Doses were selected based on in-house experience with DNA minicircles for other similar proteins (unpublished observation). Twenty-four–hour urinary albumin excretion was measured every 2 weeks for 8 weeks. ANGPT1 minicircle produced a dose-dependent reduction in UAE beginning 4 weeks after administration at the 20- and 60-μg doses. At the end of the study the area under the curve (AUC) for UAE was calculated and was significantly decreased only in the 60-μg dose group, reduced 56.3% versus the control group (Fig. 2A; results are shown from individual animals and as mean ± S.E.M.). To test for statistical significance ($P < 0.05$), a one-way ANOVA with Dunnett's multiple-comparison test versus db/db was performed.

Endothelial function was tested by vasodilation of aortic ring response to acetylcholine; a representative dose-response curve for each treatment group is shown in Supplemental Fig.1. The 60-μg ANGPT1 minicircle treatment exhibited significant restoration of the vasodilation response to acetylcholine treatment compared with the db/db control group (Fig. 2B; mean ± S.E.M.; $^{*}p < 0.05$ versus control, $^{\Lambda}p < 0.0001$ versus control as determined by AUC). The summarized data were presented as the mean percent relaxation ± S.E.M., with the EC_{50} value for each group shown in the table below the graph.

Finally, significant reductions in glomerulosclerosis (by 18.1% versus db/db control group) were also only observed in the 60-μg ANGPT1 minicircle–treated group (Fig. 2C; results are shown from individual animals and as mean ± S.E.M.) To test for statistical significance ($P < 0.05$), a one-way ANOVA with Dunnett's multiple comparison test *versus* db/db was performed. Representative histology images are also shown from an animal with glomerulosclerosis and interstitial lesion scores closest to the group mean (Fig. 2D).

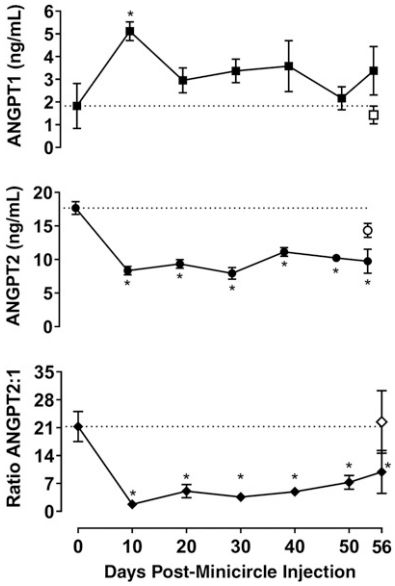

Fig. 3. Increase in circulating ANGPT1, decrease in circulating ANGPT2, and the ratio between the proteins, at the maximally efficacious dose of ANGPT1 DNA minicircle (60 μg) in a study lasting 56 days in db/db mice. Results were compared with those of an untreated db/db group (open symbol at day 56). The average concentration (C_{avg}) increase in ANGPT1 from baseline was 1.53 ng/mL.

Circulating Levels of ANGPT1 and ANGPT2 After a Single 60-mg Dose of ANPGT1 DNA-MC in db/db Mice (Fig. 3)

Using the renoprotective dose of ANGPT1 minicircle (60 μg/mouse), a study was performed to define the associated levels of the target protein in plasma. ANGPT1 minicircle was delivered into db/db mice at 8 weeks of age and blood samples were collected every 10 days post transfection. Injection of the minicircle had no appreciable effect on body weight gain in the animals; at the time of injection, body weight (group means) was 35.2 g (vehicle) *versus* 35.96 g (minicircle) and at the end of the study (56 days post–minicircle injection), the body weight was 50.87 g (vehicle) versus 49.69 g (minicircle).

Both circulating ANGPT1 and ANGPT2 were measured. As expected, and despite some variability in measured values, administration of the ANGPT1 minicircle resulted in a relatively sustained elevation in circulating ANGPT1 levels to approximately 85% above predose baseline levels (Fig. 3A), although values were only statistically elevated at Day 10 postdose. A one-way ANOVA with Dunnett's multiple comparison test versus Day 0 was performed to test for statistical significance ($P < 0.05$). The increase in ANGPT1 was biologically relevant, as evidenced by a suppression in circulating ANGPT2 levels by roughly 40% (Fig. 3B) and indicative of sustained pathway engagement. Using the same statistical methodology, ANGPT2 values were statistically reduced at each postdose time point. Mathematically, this resulted in a net reduction in the ANGPT2/1 ratio of approximately 75% versus values in untreated mice, in which, again using the same statistical methodology, the ANGPT2/1 ratio was decreased versus predose levels at each postdose time point.

Effect of the ANGPT1 Non-Neutralizing Antibody, O010, on DN Progression in db/db Uni-Nephrectomy Mice (Figs. 4 and 5)

It was previously reported that circulating ANGPT1 levels were significantly increased in cynomolgus monkeys treated with a non-neutralizing anti-ANGPT1 antibody (Zheng et al., 2018). To demonstrate the potential benefit of increasing circulating ANGPT1 levels on the renoprotective efficacy in db/db uni-nephrectomy (UNx) mice, a study was performed utilizing the same biotherapeutic molecule, termed O010.

Treatment with 10mg/kg of O010, dosed weekly in db/db UNx mice, significantly increased circulating ANGPT1 protein by 60%, but had no effect on systemic ANGPT2; in total the ANGPT2/ANGPT1 ratio was reduced by 45% (Fig. 4, A–C; results are shown from individual animals as well as mean ± S.E.M.). A Student's t test (unpaired, two-tailed) was performed to test for statistical significance ($P < 0.05$). However, no statistically significant reduction in UAE was observed either temporally or as an AUC during the course of the study (Fig. 4, D and E), including no difference between the IgG- and O010-treated db/db mice at the end of the study (week 10 in Fig. 4D).

Lack of reduction in UAE was confirmed in a second study testing O010 in db/db mice using a similar study design. In

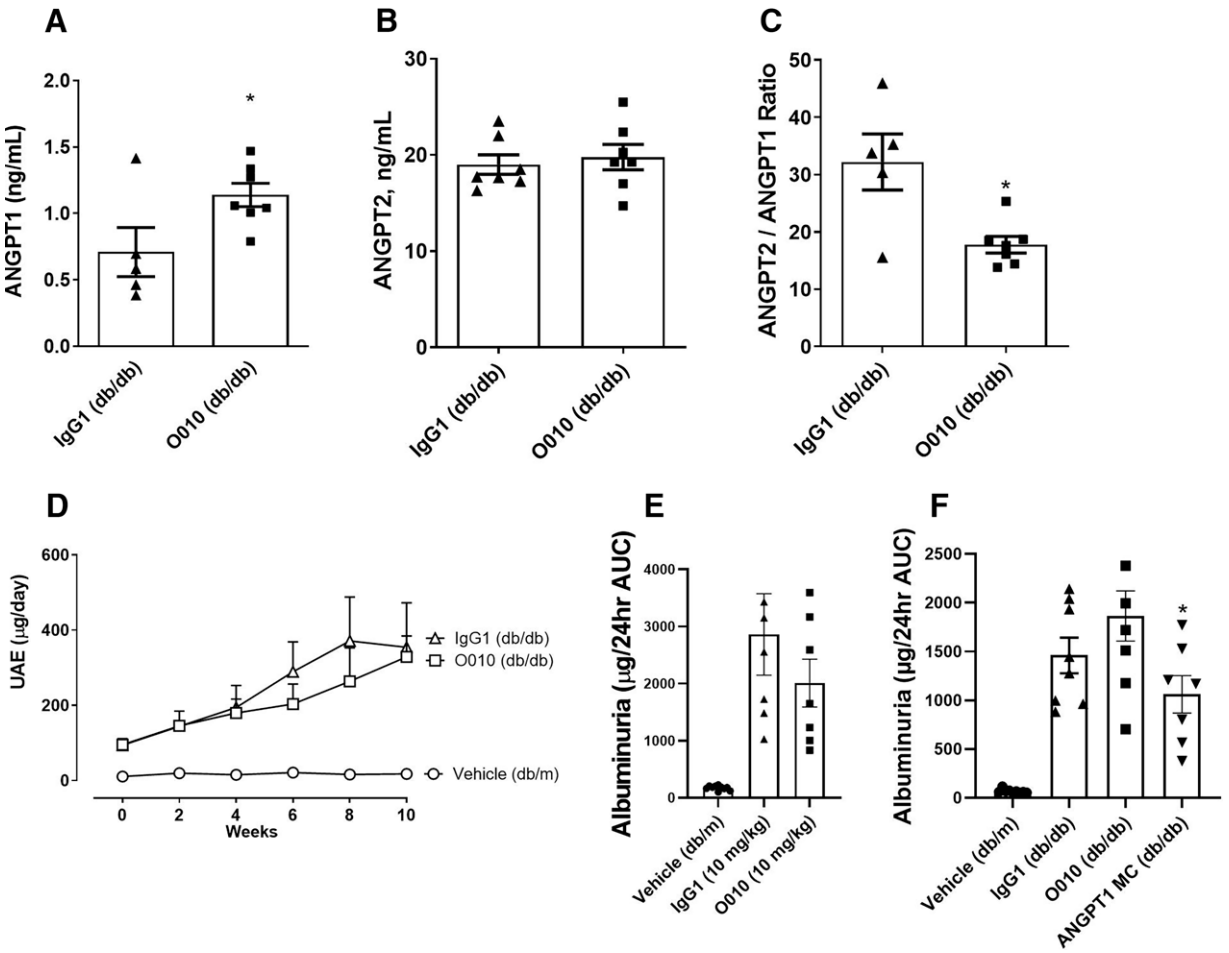

Fig. 4. Effect of a non-neutralizing antibody to ANGPT1 (O010) in db/db UNX mice on (A) plasma ANGPT1, (B) plasma ANGPT2, and (C) the ratio of ANGPT2 to ANGPT1. (D) Urinary excretion of albumin over 10 weeks. (E) Urinary excretion of albumin expressed as an AUC. (F) Urinary excretion of albumin expressed as an AUC as compared with a dose of ANGPT1 DNA minicircle (60 μg/mouse) in a follow-up study.

addition, a 60-μg ANGPT1 MC group was included as a positive control in the study. Consistent with the first study, 10 mg/kg O010 again failed to reduce urinary albuminuria compared with the IgG isotype control group. This lack of effect was in contrast with that of the ANGPT1 MC that significantly reduced albuminuria as compared with O010-treated mice (Fig. 4F; results are shown from individual animals as well as mean ± S.E.M.). To test for statistical significance ($P < 0.05$), a Student's t test (unpaired, two-tailed) was performed versus either IgG1- or O010-treated mice as appropriate.

Finally, O010 had no beneficial effect on histopathological endpoints, including incidence of glomerulosclerosis, interstitial lesion, and podocyte number quantified by IHC of p57 (Fig. 5, A–C; results are shown from individual animals and as mean ± S.E.M.). A one-way ANOVA with Dunnett's multiple comparison test versus the db/db IgG1 group was performed to test for statistical significance ($P < 0.05$). Representative histology images are shown from an animal with values closest to the group mean.

Effect of the ANGPT1 Non-Neutralizing Antibody, O010, on TIE2 Activation and Permeability in HUVECs (Fig. 6)

Failure of O010 to reduce circulating ANGPT2 protein levels in db/db UNx mice suggested the antibody may have interfered with some of ANGPT1's activity. Therefore, O010 interference of TIE2 translocation to endothelial adherens junctions and impact on endothelial cell monolayer permeability were tested using primary human endothelial cells in vitro. Activated TIE2 receptors translocated to the adherens junctions in HUVEC monolayers following treatment with recombinant ANGPT1, as shown by colocalization of pTIE2 with VE-cadherin by confocal microscopy (Fig. 6A) and an increase in quantified junctional pTIE2 levels (Fig. 6B). In contrast, when ANGPT1 treatment was performed in the presence of the ANGPT1 antibody, O010, junctional pTIE2 was substantially reduced. The summarized data are presented as the junctional pTie2 integrated density ± S.E.M. from one experiment. Statistical analysis was performed using one-way ANOVA with Dunnett's multiple comparison test. The functional consequence of ANGPT1-mediated TIE2 activation and translocation to the adherens junctions is enhanced stability of the endothelial monolayer. Thus, in vitro permeability was assessed by creating a stable HUVEC monolayer which could be disrupted by TNFα treatment (Fig. 6C). Concurrent treatment of ANGPT1 together with TNFα significantly reduced permeability compared with TNFα alone, supporting the prostability function of ANGPT1. While concomitant treatment with the IgG control had no effect, in the presence of the O010 ANGPT1 antibody the protective effect of ANGPT1 is abolished

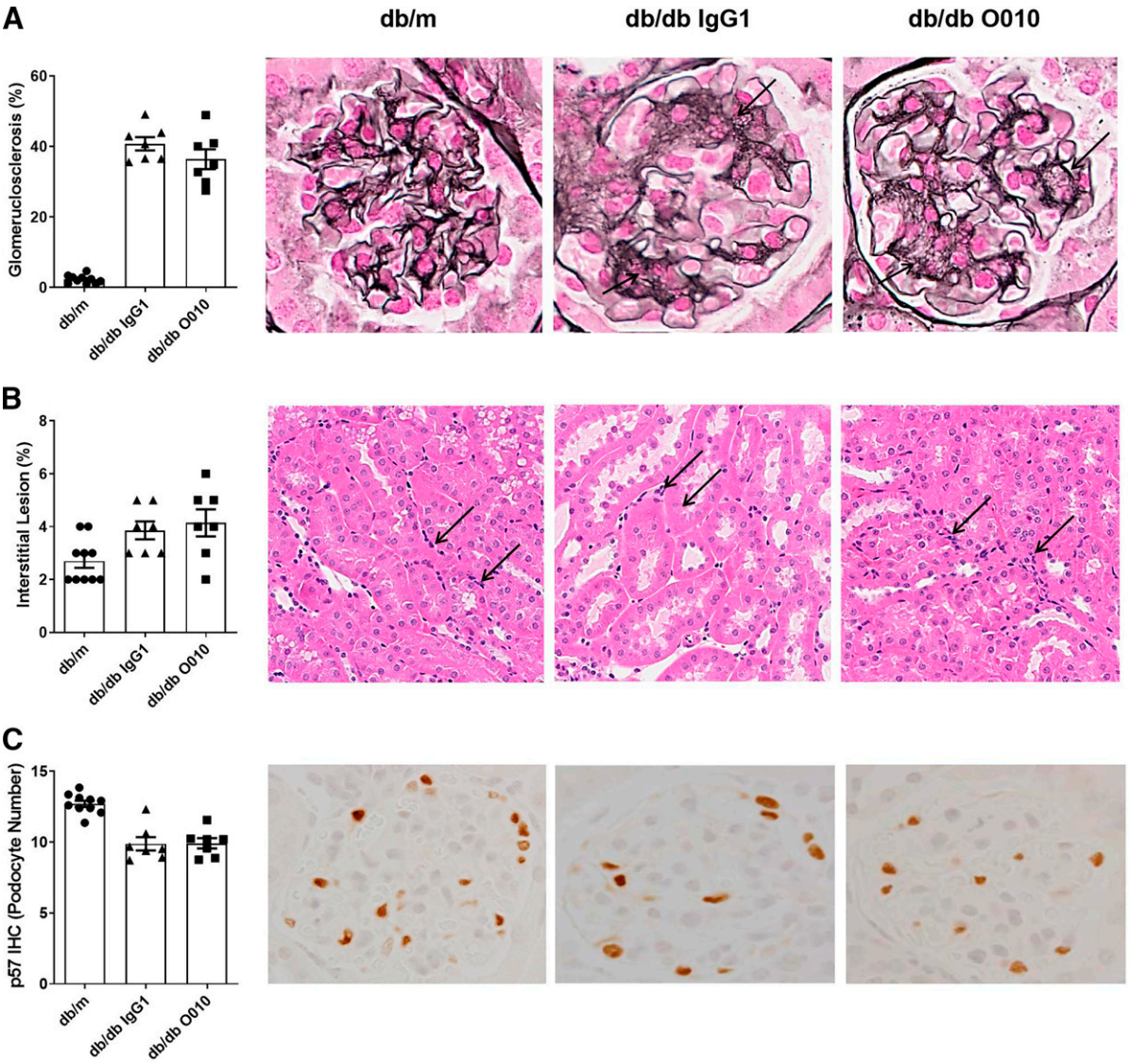

Fig. 5. Effect of O010 on renal histopathology. (A) Effect of a non-neutralizing antibody to ANGPT1 (O010) in db/db UNX mice, as shown in Figure 4, on histologic markers of chronic kidney disease including glomerular lesions in sections from vehicle (db/m), IgG1 (10 mg/kg), and O010 (10 mg/kg) mice stained by PAM. Glomerulus from vehicle shows fine mesangial matrix stained black by PAM. IgG1 glomerulus shows expanded matrix throughout the mesangium. Glomerulus from O010 mouse shows slightly less mesangial matrix expansion (arrows). (B) Interstitial lesions in sections stained by H&E; interstitial disease in all three groups was minimal, mainly showing focal hypercellularity (Arrows). The number of foci with these lesions were higher in IgG1 and O010 groups versus vehicle. (C) The results for podocyte number followed a similar trend as observed for glomerulosclerosis and interstitial assessments. Podocyte number was highest in vehicle mice; db/db mice that received IgG1 had a significant reduction in average podocyte number that was not improved with O010. db/m, vehicle.

(Fig. 6C), suggesting that the interference of the O010 antibody on pTIE2 translocation is critically detrimental to some ANGPT1 function. Data are shown from one of two independent experiments and displayed as mean ± S.E.M. Statistical analysis was performed using one-way ANOVA with Šídák's multiple comparison test, testing for 6 comparisons (Media versus TNFα, TNFα versus TNFα +Angpt1, TNFα +Angpt1 versus O010, TNFα+Angpt1 versus IgG control, TNFα versus O010, and TNFα versus IgG Control). *$P < 0.05$, **$P < 0.01$, ***$P < 0.001$, ****$P < 0.0001$.

Discussion

In the present study several unique strategies to increase ANGPT1 protein levels in the circulation of db/db mice were tested to assess potential to mitigate progression of diabetic nephropathy. Results confirmed and reproduced data demonstrating that AAV-mediated delivery of COMP-Ang1, a stable and potent variant of ANGPT1, reduces albuminuria and glomerulosclerosis in db/db mice (Lee et al., 2007). Importantly, results also demonstrate that TIE2 activation by COMP-Ang1 reduces the circulating levels of ANGPT2; it has been previously demonstrated that ANGPT1-induced activation of TIE2 increases Akt and FOXO1 signaling, which in turn negatively regulates ANGPT2 gene expression (Daly et al., 2004). Thus, in this series of studies, the use of circulating ANGPT2 levels as an indirect proxy of ANGPT1-TIE2 receptor engagement was validated.

Next, the native form of ANGPT1 was overexpressed in db/db mice using DNA minicircle, and a dose titration was

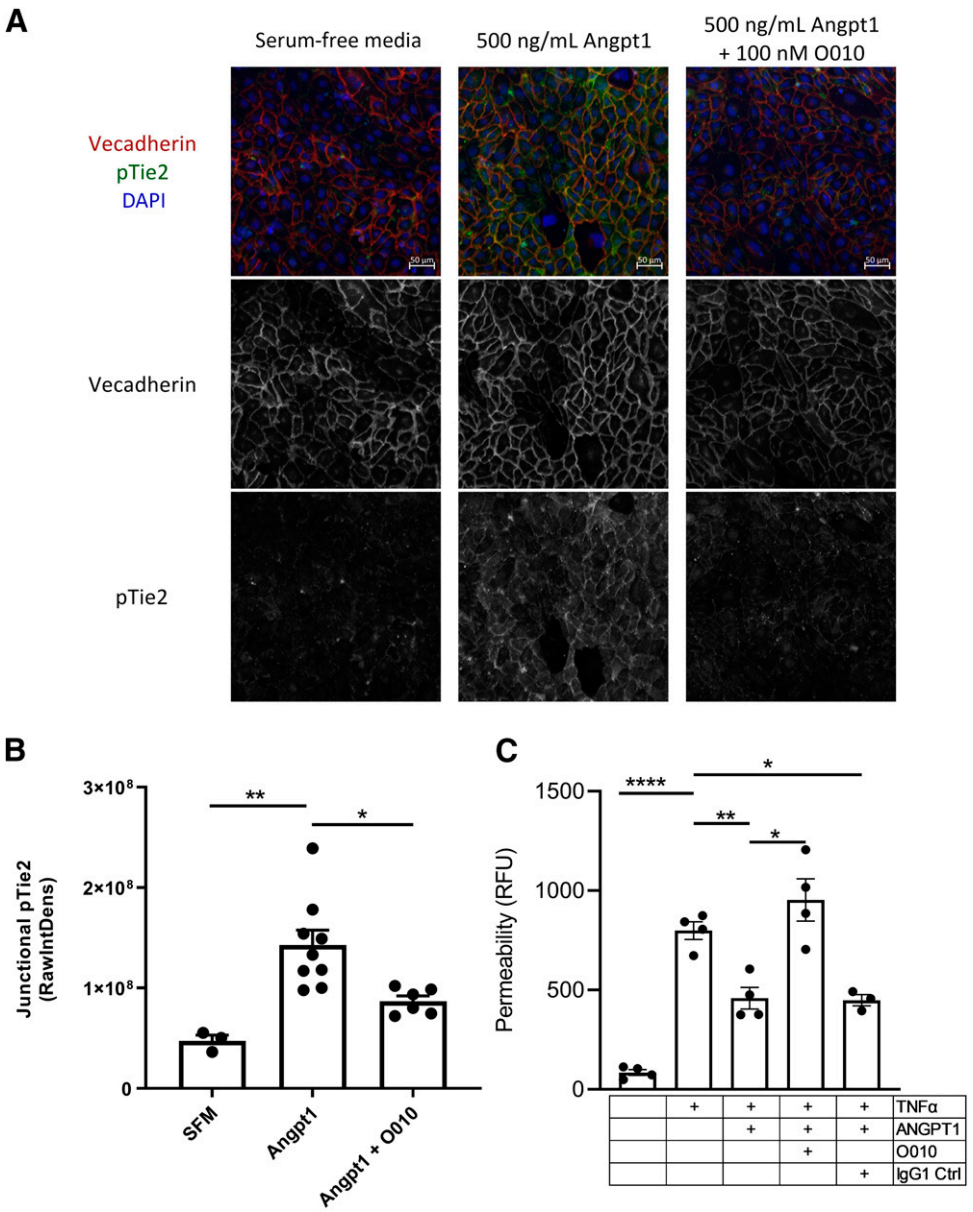

Fig. 6. Effect of O010 on ANGPT1 function in vitro. Phosphorylated TIE2 receptors within the adherens junctions in HUVECs are shown (A) by colocalization of pTIE2 (green) with VE-cadherin (red) after treatment with ANGPT1 for 30 minute, and junctional pTIE2 levels quantified (B). In vitro permeability was assessed (C) using FITC-dextran permeation across a HUVEC monolayer following 24-hour stimulation with vascular permeability factors (10 ng/mL TNFα, 200 ng/mL ANGPT1, and 100 nM of O010 or IgG1 control antibody).

performed to identify the magnitude of ANGPT1 elevation required for improvement in UACR and glomerulosclerosis in a widely accepted preclinical model of diabetic nephropathy. Results demonstrated that an 85% increase in circulating ANGPT1 was sufficient to significantly reduce UACR and the incidence of glomerulosclerosis and partially restore diabetes-induced endothelial dysfunction. Consistent with the results using COMP-Ang1 to overexpress the protein, native ANGPT1 also reduced ANGPT2 levels by approximately 40%.

Finally, the present study tested a recently described and novel biotherapeutic modality to increase endogenous ANGPT1 protein levels using a non-neutralizing anti-ANGPT1 antibody, referred to as O010, that binds within the coiled-coil domain of ANGPT1 (a site independent of the receptor binding domain) and reduces the clearance, resulting in increased circulating concentrations of ANGPT1. It was previously shown that the O010 antibody does not interfere with ANGPT1 binding to TIE2, nor does it reduce phosphorylated AKT signaling in a cell line (Zheng et al., 2018). Furthermore, this antibody significantly increased circulating ANGPT1 levels in healthy cynomolgus monkeys (Zheng et al., 2018), which was consistent with the targeted mechanism-of-action. The present study also demonstrated an increase in circulating ANGPT1 with O010 in db/db UNx mice, however, the molecule failed to reduce renal injury endpoints, including no effect on albuminuria or histopathology scores, including the incidence of glomerulosclerosis and interstitial lesions.

Podocytes play a key role in the preservation of normal glomerular structure and function (Pagtalunan et al., 1997) and are the principal source of ANGPT1 release in the kidney where the protein colocalizes with nephrin in the foot process (Satchell et al., 2002). It is well accepted that podocyte loss is associated with the progression of glomerular diseases both in humans and in experimental models of glomerular injury (Matsusaka et al., 2005). Confirming the importance of and delicate balance in the ANGPT1-ANGPT2-Tie2 axis in maintaining glomerular integrity, Davis et al., (1996) demonstrated that inducible ANGPT2 expression in the podocyte itself resulted in significant albuminuria, glomerular endothelial apoptosis, and a loss of nephrin proteins critical for the integrity of the filtration barrier. In this study, animals treated with O010 also failed to protect against podocyte loss, an effect likely contributing to the lack of benefit on albuminuria.

The disconnect in efficacy outcomes between a strategy using ANGPT1 overexpression and treatment with a stabilizing antibody was therefore interrogated. In both studies a 60%–85% increase in circulating ANGPT1 was achieved. However, it should be noted that the absolute level of systemic ANGPT1 in each study was different; using the ANGPT1 minicircle average concentration (C_{avg}), protein levels increased to 1.53 ng/mL, while with O010 treatment values were slightly less, at 1.14 ng/mL. This difference alone may have contributed, at least in part, to the lack of efficacy to reduce renal outcomes with O010.

However, no reduction in circulating ANGPT2 protein levels was observed after treatment with O010 in db/db UNx mice, suggesting that the ANGPT1-O010 complex may interfere with activation of the TIE2 receptor and, consequently, downstream signaling and renoprotection. Of note, in healthy cynomolgus monkeys, O010 also failed to reduce circulating ANGPT2 levels (Zheng et al., 2018), although in that study the impact of the biotherapeutic on disease outcomes was not interrogated. It is plausible that the lack of ANGPT2-suppression by the molecule may be due to the failure to increase the absolute circulating ANGPT1 levels with O010 treatment to the same extent as observed with the ANGPT1 minicircle in both cynomolgus monkeys and db/db mice.

An alternative or additional explanation explored experimentally centered on O010 interference with TIE2 translocation to endothelial adherens junctions. If true, O010-bound ANGPT1 would fail to stabilize the glomerular endothelial cells of the filtration barrier. Indeed, it has been shown that TIE2 signaling is dependent on both receptor and ligand localization (Fukuhara et al., 2008; Saharinen et al., 2008). Promotion of vascular quiescence is regulated by ANGPT1-induced translocation of TIE2 to cell-cell contacts, while angiogenesis is promoted by extracellular matrix-anchored ANGPT1 (Fukuhara et al., 2010). Thus, to investigate further, confocal microscopy was used to demonstrate that O010 in fact prevented the translocation of pTIE2 to VE-cadherin$^+$ junctions and blocked the ability of ANGPT1 to stabilize endothelial cell monolayers in vitro. In total, these observations likely more accurately explain the lack of renoprotection with O010, despite an effect of the molecule to increase the systemic levels of the ANGPT1 protein.

This complete body of work supports the belief that increasing ANGPT1-TIE2 signaling has the potential to be beneficial in the treatment of diabetic kidney disease. Multiple therapeutic strategies are envisioned, including agonizing the TIE2 receptor directly in a localized manner (i.e., at glomerular endothelial cells), precipitating localized ANGPT1 production to promote glomerular endothelial TIE2 activation, or by increasing ANGPT1 concentrations in the circulation in a manner not interfering with TIE2 junctional translocation. Although the present data, using a novel approach to promote half-life extension of the protein, was negative in terms of efficacy benefit, it is undetermined whether the effect is antibody- or epitope-specific, or inherent to all ANGPT1 antibodies employing a similar approach. It is essential that the complex biology around TIE2 signaling and localization be considered in the development of future ANGPT1-elevating therapeutics.

Authorship Contributions

Participated in research design: Sun, Bartlett, Zheng, Grant, Kerr, Fryer.

Conducted experiments: Sun, Bartlett, Bigwarfe, MacDougall, Berger, McHugh, Chen, Zhang, Carpenter, Robinson.

Contributed new reagents or analytic tools: Zheng, Miglietta, Lamla.

Performed data analysis: Sun, Bartlett, Kerr, Qian, McHugh, Fryer.

Wrote or contributed to the writing of the manuscript: Sun, Bartlett, Kerr, Qian, Fryer.

References

Aschauer DF, Kreuz S, and Rumpel S (2013) Analysis of Transduction Efficiency, Tropism and Axonal Transport of AAV Serotypes 1, 2, 5, 6, 8 and 9 in the Mouse Brain. *PLoS One* **8**:e73610.

Bell S, Fletcher EH, Brady I, Looker HC, Levin D, Joss N, Traynor JP, Metcalfe W, Conway B, Livingstone S et al.; Scottish Diabetes Research Network and Scottish Renal Registry (2015) End-stage renal disease and survival in people with diabetes: a national database linkage study. *QJM* **108**:127–134.

Cho CH, Kammerer RA, Lee HJ, Yasunaga K, Kim KT, Choi HH, Kim W, Kim SH, Park SK, Lee GM et al. (2004) Designed angiopoietin-1 variant, COMP-Ang1, protects against radiation-induced endothelial cell apoptosis. *Proc Natl Acad Sci USA* **101**:5553–5558.

Daly C, Wong V, Burova E, Wei Y, Zabski S, Griffiths J, Lai KM, Lin HC, Ioffe E, Yancopoulos GD et al. (2004) Angiopoietin-1 modulates endothelial cell function and gene expression via the transcription factor FKHR (FOXO1). *Genes Dev* **18**:1060–1071.

Davis S, Aldrich TH, Jones PF, Acheson A, Compton DL, Jain V, Ryan TE, Bruno J, Radziejewski C, Maisonpierre PC et al. (1996) Isolation of angiopoietin-1, a ligand for the TIE2 receptor, by secretion-trap expression cloning. *Cell* **87**:1161–1169.

Md Dom ZI, Satake E, Skupien J, Krolewski B, O'Neil K, Willency JA, Dillon ST, Wilson JM, Kobayashi H, Ihara K et al. (2021) Circulating proteins protect against renal decline and progression to end-stage renal disease in patients with diabetes. *Sci Transl Med* **13**:eabd2699.

Fiedler U and Augustin HG (2006) Angiopoietins: a link between angiogenesis and inflammation. *Trends Immunol* **27**:552–558.

Fiedler U, Scharpfenecker M, Koidl S, Hegen A, Grunow V, Schmidt JM, Kriz W, Thurston G, and Augustin HG (2004) The Tie-2 ligand angiopoietin-2 is stored in and rapidly released upon stimulation from endothelial cell Weibel-Palade bodies. *Blood* **103**:4150–4156.

Fukuhara S, Sako K, Noda K, Zhang J, Minami M, and Mochizuki N (2010) Angiopoietin-1/Tie2 receptor signaling in vascular quiescence and angiogenesis. *Histol Histopathol* **25**:387–396.

Fukuhara S, Sako K, Minami T, Noda K, Kim HZ, Kodama T, Shibuya M, Takakura N, Koh GY, and Mochizuki N (2008) Differential function of Tie2 at cell-cell contacts and cell-substratum contacts regulated by angiopoietin-1. *Nat Cell Biol* **10**:513–526.

Futrakul N, Butthep P, and Futrakul P (2008) Altered vascular homeostasis in chronic kidney disease. *Clin Hemorheol Microcirc* **38**:201–207.

Ghaderian SB, Hayati F, Shayanpour S, and Beladi Mousavi SS (2015) Diabetes and end-stage renal disease; a review article on new concepts. *J Renal Inj Prev* **4**:28–33.

Jeansson M, Gawlik A, Anderson G, Li C, Kerjaschki D, Henkelman M, and Quaggin SE (2011) Angiopoietin-1 is essential in mouse vasculature during development and in response to injury. *J Clin Invest* **121**:2278–2289.

Kim SR, Lee KS, Park SJ, Min KH, Lee KY, Choe YH, Hong SH, Koh GY, and Lee YC (2008) Angiopoietin-1 variant, COMP-Ang1 attenuates hydrogen peroxide-induced acute lung injury. *Exp Mol Med* **40**:320–331.

Lee S, Kim W, Moon SO, Sung MJ, Kim DH, Kang KP, Jang KY, Lee SY, Park BH, Koh GY et al. (2007) Renoprotective effect of COMP-angiopoietin-1 in db/db mice with type 2 diabetes. *Nephrol Dial Transplant* **22**:396–408.

Matsusaka T, Xin J, Niwa S, Kobayashi K, Akatsuka A, Hashizume H, Wang QC, Pastan I, Fogo AB, and Ichikawa I (2005) Genetic engineering of glomerular sclerosis in the mouse via control of onset and severity of podocyte-specific injury. *J Am Soc Nephrol* **16**:1013–1023.

Pagtalunan ME, Miller PL, Jumping-Eagle S, Nelson RG, Myers BD, Rennke HG, Coplon NS, Sun L, and Meyer TW (1997) Podocyte loss and progressive glomerular injury in type II diabetes. *J Clin Invest* **99**:342–348.

Reed BY and Schrier RW (2011) Circulating angiopoietin-1 could be confounded by ex vivo platelet activation. *Kidney Int* **79**:687–688.

Ryu JK, Kim WJ, Koh YJ, Piao S, Jin HR, Lee SW, Choi MJ, Shin HY, Kwon MH, Jung K et al. (2015) Designed angiopoietin-1 variant, COMP-angiopoietin-1, rescues erectile function through healthy cavernous angiogenesis in a hypercholesterolemic mouse. *Sci Rep* **5**:9222.

Saharinen P, Eklund L, Miettinen J, Wirkkala R, Anisimov A, Winderlich M, Nottebaum A, Vestweber D, Deutsch U, Koh GY et al. (2008) Angiopoietins assemble distinct Tie2 signalling complexes in endothelial cell-cell and cell-matrix contacts. *Nat Cell Biol* **10**:527–537.

Satchell SC, Harper SJ, Tooke JE, Kerjaschki D, Saleem MA, and Mathieson PW (2002) Human podocytes express angiopoietin 1, a potential regulator of glomerular vascular endothelial growth factor. *J Am Soc Nephrol* **13**:544–550.

Strobel B, Duechs MJ, Schmid R, Stierstorfer BE, Bucher H, Quast K, Stiller D, Hildebrandt T, Mennerich D, Gantner F et al. (2015) Modeling Pulmonary Disease Pathways Using Recombinant Adeno-Associated Virus 6.2. *Am J Respir Cell Mol Biol* **53**:291–302.

Uemura A, Ogawa M, Hirashima M, Fujiwara T, Koyama S, Takagi H, Honda Y, Wiegand SJ, Yancopoulos GD, and Nishikawa S (2002) Recombinant angiopoietin-1 restores higher-order architecture of growing blood vessels in mice in the absence of mural cells. *J Clin Invest* **110**:1619–1628.

Yuan HT, Tipping PG, Li XZ, Long DA, and Woolf AS (2002) Angiopoietin correlates with glomerular capillary loss in anti-glomerular basement membrane glomerulonephritis. *Kidney Int* **61**:2078–2089.

Zheng C, Toth J, Bigwarfe T, MacDougall M, Jerath K, Bovat K, Smith J, Sun P, Hayes D, Fryer R et al. (2018) Non-neutralizing antibodies increase endogenous circulating Ang1 levels. *MAbs* **10**:1260–1268.

Address correspondence to: Dr. Ryan M. Fryer, Boehringer Ingelheim Pharmaceuticals, Inc. 900 Ridgebury Road, Ridgefield, CT 06877-0368. E-mail: ryan.fryer@boehringer-ingelheim.com

Effect of Novel Biotherapeutic Elevating Angiopoietin 1 on Progression of Diabetic Nephropathy in Diabetic/Obese Mice

Peng Sun*, Christina S. Bartlett*, Chao Zheng, Tammy Bigwarfe, Joshuaine M. Grant, Margit MacDougall, Valentina Berger, Steven Kerr, Hu Sheng Qian, Mark McHugh, Hongxing Chen, Xiaomei Zhang, Miranda L. Carpenter, Heather N. Robinson, John Miglietta, Thorsten Lamla, Ryan M. Fryer

Cardiometabolic Diseases Research (CB, PS, MM, VB, SK, HQ, MM, HC, AZ, MC, HR, RF), Biotherapeutic Discovery (CZ, JM), Biotherapeutic Pharmacokinetics (TB, JG), Target Discovery Research (TL)

Boehringer Ingelheim Pharmaceuticals Inc., Ridgefield, CT, USA 06877

S1

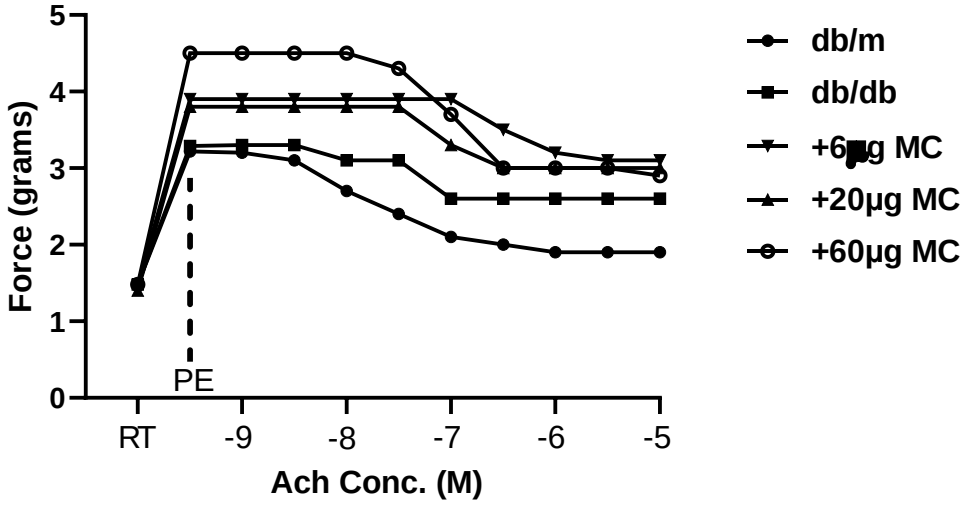

	db/m	+60µg MC	+20µg MC	+6µg MC	db/db
PE Cont. (g)	4.03 ± 0.26	3.21 ± 0.26	3.79 ± 0.26	3.88 ± 0.28	3.79 ± 0.28

Supplemental Figure 1. A representative acetylcholine dose response curve in aortic rings from each treatment group. Mean baseline values following phenylephrine contraction are listed immediately below the figure. Values are shown as mean ± S.E.M. RT, resting tension, PE, phenylephrine.